Morris A, Robertson AHF, Anderson MW & Hodgson E 2016 'Did the Kyrenia Range of northern Cyprus rotate with the Troodos-Hatay microplate during the tectonic evolution of the eastern Mediterranean?' *INTERNATIONAL JOURNAL OF EARTH SCIENCES* 105, (1) 399-415

*The final publication is available at Springer via http://dx.doi.org/10.1007/s00531-015-1208-9*

# Did the Kyrenia Range of northern Cyprus rotate with the Troodos-Hatay microplate during the tectonic evolution of the eastern Mediterranean?

Antony Morris[1], Alastair H. F. Robertson[2], Mark W. Anderson[1] & Emma Hodgson[1,3]

[1]School of Geography, Earth and Environmental Sciences, Plymouth University, Drake Circus, Plymouth PL4 8AA, UK
[2]School of GeoSciences, Grant Institute, University of Edinburgh, James Hutton Road, Edinburgh EH9 3FE, UK
[3]now at Geomagnetism Lab, School of Environmental Sciences, University of Liverpool, Oliver Lodge Laboratories, Oxford Road, Liverpool L69 7ZE, UK

**Abstract**

Previous palaeomagnetic studies have allowed the recognition of a distinctive area of Neotethyan oceanic rocks, including the Troodos ophiolite in Cyprus and the Hatay ophiolite to the east in southern Turkey, that underwent 90° of anticlockwise rotation between Late Cretaceous (Campanian) and Early Eocene time. The southern and western boundaries of this rotated Troodos-Hatay microplate have been inferred to lie within, or adjacent to, zones of deformed oceanic and continental margin rocks that are now exposed in southern and western Cyprus; however, the northern boundary of the microplate remains undefined. Relevant to this problem, palaeomagnetic data are presented here from basaltic lavas exposed along the Kyrenia Range, mostly from Late Cretaceous (Maastrichtian) sites and one Eocene site. A positive inclination-only fold test demonstrates that remanences are pre-deformational in age, and positive conglomerate tests show that magnetic remanences were acquired before Late Eocene-Early Oligocene time, together suggesting that primary magnetizations are preserved. Data from the eastern Kyrenia Range and the Karpas Peninsula (the easternmost extension of the Kyrenia Range) document significant relative tectonic rotation between these localities, with no rotation in the eastern range versus 30° of anticlockwise rotation of the Karpas Peninsula. Unfortunately, palaeomagnetic sites from the western Kyrenia range did not yield tectonically interpretable magnetization directions, probably due to complex poly-phase thrusting and folding, and the central range also yielded no interpretable data. However, the available palaeomagnetic data are sufficient to demonstrate that the Kyrenia terrane underwent a separate rotation history to the Troodos-Hatay microplate and also implies that the northern boundary of the Troodos-Hatay microplate was located between the Troodos ophiolite and the Kyrenia Range. The former microplate margin has since been overridden and concealed by two phases of southward thrusting and folding of the Kyrenia Range units (Mid-Eocene; latest Miocene-earliest Pliocene). The likely cause of the anticlockwise rotation affecting the Karpas Peninsula, and by implication the curvature of the Kyrenia Range as a whole, relates to regional late-stage subduction and diachronous continental collision. The Southern Neotethys sutured in SE Turkey during the Early Miocene, whereas a relict ocean basin remained further west in the easternmost Mediterranean, allowing a

remnant N-dipping subduction zone to retreat southwards and so induce the present-day arcuate shape of the Kyrenia Range.

**Key words:** palaeomagnetism; rotation; Kyrenia Range; Troodos; Cyprus; eastern Mediterranean; Tethys; tectonics; microplate

**Introduction**

Vertical-axis rotations of crustal blocks of different scales play an important role in the tectonic evolution of oceanic basins and their margins (e.g. Morris and Tait 2003). An excellent example is the Troodos ophiolite in Cyprus, which formed by sea-floor spreading above a subduction zone c. 90 million years ago (e.g. Mukasa and Ludden 1987; Robertson and Xenophontos 1993). Afterwards, between c. 75 and c. 50 million years ago (Late Campanian-Early Eocene), the Troodos ophiolite underwent a 90° anticlockwise rotation as an inferred microplate (Moores and Vine 1971; Clube et al. 1985; Clube and Robertson 1986; Morris et al. 1990). The likely cause of the rotation was the collision of a subduction zone (above which the Troodos formed) with the step-shaped N Africa-Levant margin to the south (Robertson 1990; Morris et al. 2006; Inwood et al. 2009). A key aim has been to identify the boundaries of the rotated microplate and so delineate the size and shape of the rotated body of oceanic crust. The western and southern boundaries of the rotated microplate are believed to be located within, or near, units of accretionary melange and continental margin origin, notably the Mamonia Complex in W Cyprus (Clube and Robertson 1986; Robertson 1990; Morris et al. 1998). More recent palaeomagnetic studies in southern Turkey suggest that the adjacent Late Cretaceous Hatay ophiolite formed a part of the rotated microplate (Inwood et al. 2009). An important question, which is addressed here, is the location of the northern boundary of the combined Troodos-Hatay microplate.

The Troodos ophiolite is currently bounded to the north by the Kyrenia Range, as shown Figure 1. This is the obvious place to test for the northern boundary of the rotated microplate. Unlike the Troodos and Hatay ophiolites, the Kyrenia Range is made up of strongly deformed continental margin lithologies of Late Palaeozoic to Holocene age (Ducloz, l972; Baroz, l979; Robertson and Woodcock 1986). The regional trend of the Kyrenia Range is approximately east-west, parallel to the structural grain of comparable continental units in southern Turkey (MTA 2002). It has, therefore, been generally assumed that the Kyrenia Range is unlikely to have undergone major tectonic rotation unlike the Troodos ophiolite (Robertson 1998). If correct, the northern boundary of the microplate should lie somewhere between the Troodos ophiolite and the Kyrenia Range. The rotation of the Troodos ophiolite is known to have ended by c. 50 Ma (Early Eocene) (Clube et al. 1985; see also Morris 1996). Since that time, the Kyrenia Range has experienced two important phases of southward thrusting and related folding during Mid-Eocene and latest Miocene-earliest Pliocene time, which need to be taken into account when considering the location of the microplate boundary.

On a regional scale, the Kyrenia Range is known to link up eastwards with the Misis Mountains of coastal southern Turkey (Kelling et al. 1987; Kempler and Garfunkel 1994; Vidal et al. 2000; Robertson et al. 2004). The Kyrenia Range extends westwards some distance offshore (Calon et al. 2005), but its termination in this direction remains uncertain (see Glover and Robertson 1998; Robertson et al. 2003; Zitter et al. 2003; Aksu et al. 2009). Late Cretaceous ophiolitic rocks, comparable with the Troodos ophiolite, are exposed onshore in the

Antalya region but these are strongly deformed and have not been studied palaeomagnetically (e.g. see Poisson 1977; Robertson and Woodcock 1982; Bağcı et al., 2009).

The main aim of this paper is to present palaeomagnetic data from basic extrusive igneous rocks that effectively test whether or not the Kyrenia Range formed a part of the Troodos-Hatay microplate. The secondary aim is to determine whether the Kyrenia Range has been affected internally by any smaller scale vertical-axis tectonic rotations and hence to consider the cause of the arcuate shape of the Kyrenia Range (Fig. 1), specifically whether this is an original palaeogeographic feature or the result of vertical axis rotation(s) during tectonic emplacement.

Fieldwork was carried out throughout the western, central and eastern segments of the Kyrenia Range plus the adjacent Karpas Peninsula during spring 2006. Preliminary palaeomagnetic results were presented by Hodgson et al. (2006). More recently, a considerable amount of stratigraphical, sedimentological and structural work has been published on the Kyrenia Range (McCay and Robertson 2012, 2013; McCay et al. 2013; Robertson et al. 2012, 2014; see also Robertson and Kinnaird, this volume), which allows a detailed interpretation of the palaeomagnetic results in the regional tectonic setting.

## Along-strike variation in the structure of the Kyrenia Range

The Kyrenia Range has an overall arcuate shape as delineated by the overall trend in the strike of the major lithological units. The range is traditionally subdivided into four contiguous units: the western range, the central range, the eastern range and the Karpas Peninsula (Fig. 1), all of which were palaeomagnetically sampled. The strike is generally WNW-ESE in the western and central range until longitude c. 33° 30' (within the central range), where it swings (over several kilometres) to a c. ENE-WSW direction which gradually becomes more NE-SW-trending within the eastern range, the Karpas Peninsula and the offshore extension of the lineament.

The central range is the simplest segment structurally as it is dominated by a series of south-verging thrust sheets (see representative cross-section in Fig. 1), which include Maastrichtian and Eocene basalts sampled in this study (Baroz 1979). Both ends of the central range are bounded by transverse fault lineaments (Robertson and Kinnaird, this volume). The relative structural simplicity is the result of the dominance of structurally competent Late Triassic-Cretaceous meta-platform carbonates (Baroz 1979; Robertson and Woodcock, l986). Accessible outcrops were mainly restricted to small, deformed sequences in the south, not far above the Kythrea Fault, which is a major thrust located near the southern front of the Kyrenia Range (Fig. 1). More extensive outcrops of Maastrichtian-Eocene basalt occur in higher thrust sheets in the north of the range, but these were too difficult to access and sample palaeomagnetically. Also, many of these outcrops are strongly weathered.

The eastern range is geologically diverse as it includes large outcrops of structurally incompetent Eocene sedimentary melange (‘olistostrome’). In some areas the eastern Kyrenia range has experienced tight tectonic imbrication and variable-scale folding (Baroz 1979; Robertson et al. 2014). The eastern range includes coherent successions of Maastrichtian-Eocene basaltic rocks, typically tens of metres thick in individual exposures; these were sampled palaeomagnetically in several areas along the southern front of the range. In some areas, younging directions determined from pillow morphologies indicate that lavas are locally structurally overturned.

The eastern Kyrenia range extends eastwards without a structural break into the Karpas Peninsula, in which a reduced range of units is exposed, largely of Neogene age. The western part of the Karpas Peninsula includes an unusually thick (up to several hundred metres) sequence of structurally coherent pillow basalts of Maastrichtian age (Robertson et al. 2012; McCay and Robertson 2013). These are relatively coherent stratigraphically and as such constituted a key palaeomagnetic sampling locality.

Lastly, the western range is the most complex segment structurally. Like the eastern range and the Karpas Peninsula, it lacks thick, structurally competent Mesozoic meta-platform carbonates. The core of the outcrop is dominated by relatively incompetent Late Cretaceous volcanic rocks, predominantly siliceous extrusives, that are rare elsewhere (Baroz 1980; Huang et al. 2007; Huang 2008; Robertson et al. 2012). There are also relatively thick (up to c. 100 m) thrust-imbricated sequences of Maastrichtian-Eocene basalts and pelagic carbonates. In addition, due to the combined effects of Mid-Eocene and latest Miocene-earliest Pliocene southward thrust imbrication, the volcanic-sedimentary succession is deformed into major (up to km-scale) southward-vergent recumbent folds (Baroz, l979; Robertson et al. 2012). As a result, most of the outcrops are strongly deformed and three of the four sites sampled in this area are overturned

## Palaeomagnetic sampling and methods

The Kyrenia Range exposes sequences of basic extrusive igneous rocks, which are unmetamorphosed and so well suited to palaeomagnetic analysis (Ducloz 1972; Baroz 1980; Robertson and Woodcock 1986; Huang et al. 2007; Huang 2008). The lavas are well dated using microfossils within depositionally interbedded pelagic carbonates (Robertson et al. 2012). The extrusives are commonly pillowed such that stratigraphical way up can usually be determined. In many places the interbedded pelagic carbonates allow palaeohorizontal surfaces to be accurately determined. We sampled Maastrichtian-Eocene basaltic lavas exposed at 28 sites along the Kyrenia Range in the four structural segments of the Kyrenia Range (outlined above) for palaeomagnetic analyses in order to quantify any tectonic rotations that have affected the range. An average of eight samples per site were drilled *in situ* using a portable petrol-driven rock drill following standard palaeomagnetic procedures. Core samples were orientated using both magnetic and sun compasses. At two sampling sites, the Maastrichtian pillow lavas were impossible to drill because of closely spaced cooling-related fractures, and these were instead sampled by collecting small, individual, joint-bounded, orientated hand samples. Sampling was restricted to exposures that showed consistent palaeohorizontal indicators as represented by the bedding in associated laterally continuous pelagic sediments or the consistent orientation of flow surfaces in coherent sequences of pillowed or sheet lava flows. The orientations of the palaeohorizontal indicators were measured in the field to an accuracy of ± 5°. With the aim of carrying out a conglomerate test, samples of basaltic-diabasic clasts were also collected from the basal conglomerates of the Bellapais (Beylerbey) Formation (Late Eocene-Early Oligocene; Fig. 2) at two sites. Drill cores could not be obtained from these clasts owing to their small size and the friable nature of the sedimentary matrix. The local field relations of extrusive and conglomeratic rocks sampled is illustrated using field photographs in Fig. 3. Locations of all 30 sampling sites are shown in Fig. 1. Of these, 18 sites (16 in lavas and two in conglomerates) yielded reliable data, as described below.

Natural remanences were measured in the Plymouth University Palaeomagnetic Laboratory using a Molspin fluxgate spinner magnetometer (noise level = 0.05 x $10^{-3}$ A/m, for an 11 $cm^3$ specimen). The small hand samples from the highly fractured pillow lavas and the conglomerate clast samples were trimmed and mounted inside plastic pots and then measured using a Molspin large aperture spinner magnetometer designed for analysis of irregularly shaped archaeomagnetic samples. At all sites, samples were subjected to both stepwise alternating field (AF) and thermal demagnetization. Characteristic remanent magnetizations (ChRMs) were found using orthogonal vector plots and principal component analysis (Kirschvink 1980) and site mean remanence directions were computed using Fisherian statistics (Fisher 1953). Supporting rock magnetic analyses were performed on selected samples. Stepwise acquisition of isothermal remanent magnetization (IRM) was used to determine coercivity spectra and measurement of the variation of low field magnetic susceptibility with temperature (performed using an AGICO KLY3-S system with furnace attachment) was used to determine Curie temperatures.

## Results and analysis

### *Magnetic mineralogy and palaeomagnetic results*

IRM acquisition curves rise steeply to generally reach saturation by fields of 100-300 mT (Fig. 4). In all cases, histograms of the rate of change of IRM acquisition suggest that low coercivity minerals are dominant. Unblocking temperatures of NRMs are predominantly between 560-580°C. These data are consistent with the presence of magnetite/Ti-poor titanomagnetite within these rocks. These phases may have evolved from more Ti-rich primary titanomagnetite phases by deuteric oxidation during initial cooling. In some samples, variations in low field magnetic susceptibility with temperature reveal complex heating curves showing two peaks (Fig. 4). The highest temperature peak represents a Hopkinson peak (Dunlop and Ozdemir 1997) just below a final Curie temperature corresponding to that of magnetite. The lower temperature peak at approximately 300°C suggests presence of titanomaghemite (possibly formed naturally from a titanomagnetite precursor phase by low temperature seafloor alteration; Xu et al. 1997) which inverts at higher temperatures in the laboratory, resulting in the production of new magnetite and an increase in low field susceptibility following cooling to room temperature (Fig. 4).

Stable characteristic remanent magnetization (ChRM) components with maximum angular deviations (Kirschvink 1980) of < 10° were isolated at 23 sites following removal of minor secondary components during initial demagnetization. Typical examples of demagnetization behaviour are shown in Fig. 5. Most samples are dominated by univectorial ChRM components that decay to the origin. Both AF and thermal demagnetization experiments yielded identical remanence directions (see samples KR2201 and KR2206 in Fig. 5). The remaining seven sites displayed unstable behaviour during demagnetization yielding insufficient samples with statistically acceptable linearity during principal component analysis (Kirschvink 1980). After assessment of distributions of ChRM data at site-level, five further sites were rejected (two with statistically unreliable mean directions (i.e. with Fisherian statistics with $\alpha_{95} \geq 15°$, $K \leq 15$) and three where ChRM directions formed a girdle distribution (suggesting variation between samples in the degree of removal of secondary components)). These were excluded from further analysis. Mean directions and associated statistics from the remaining 18 sites are listed in Table 1.

Data from the western and central ranges show well-defined mean directions of magnetization at the site level that are unrelated to the present day field direction (Table 1), but no directional consistency between sites at the locality level. These data are considered to be uninterpretable in terms of tectonic rotations for reasons discussed below. In contrast, data from the eastern range and Karpas Peninsula are consistent at the locality level (Table 1). The *in situ* and tilt corrected magnetic remanences from these sites are shown on stereographic equal area projections in Figure 6. Following tilt correction, magnetizations in the eastern range are of mixed polarity whereas those in the Karpas Peninsula are consistently of normal polarity. Directions are unrelated to the present-day geocentric axial dipolar field in the Kyrenia region (Fig. 6), suggesting that ancient magnetizations are preserved.

*Averaging of palaeosecular variation of the geomagnetic field and the timing of magnetization acquisition*

For meaningful geological interpretation of the palaeomagnetic data it is necessary to demonstrate that magnetic remanences in the sampled basaltic lavas: (i) provide adequate sampling of palaeosecular variation (PSV) of the geomagnetic field, so that differences between observed directions of magnetization and appropriate reference directions may confidently be considered to be solely of tectonic origin; and (ii) are pre-deformational in age and were acquired during or shortly after initial crystallisation rather than during any regional remagnetization event.

Data from basaltic lavas of the Karpas Peninsula locality come from eight sites with statistically reliable site mean directions (Fig. 6; Table 1). At each site, each core sample was collected from a separate individual pillow (with the exception of Site KR21 where a thick sheet flow was sampled). Although this approach may partially average out PSV at the site level, it is probable that site level data still represent spot readings of the geomagnetic field during eruption of the lavas. Averaging of site mean directions at the locality-level is likely to be much more effective at sampling PSV adequately. This can be tested statistically using the methodology of Deenen et al. (2011), who performed a bootstrap analysis of samples with different $N$ values drawn from PSV models in order to provide upper and lower 95% confidence bounds on $A_{95}$ values of virtual geomagnetic pole (VGP) distributions that adequately average PSV. VGPs calculated from the Karpas Peninsula data have an overall $A_{95}$ of 10.7°. This falls between the critical values for $N$ = 8 of $A_{95max}$ = 22.1° and $A_{95min}$ = 7.4° (Deenen et al. 2011), demonstrating that these data account for expected PSV and may therefore be employed in tectonic analysis. Data from the eastern range locality are unfortunately too sparse to allow a similar statistical analysis ($N$ = 3). However, we note that these sites record both normal and reversed polarities of the geomagnetic field (Fig. 6; Table 1) indicating remanences were acquired over a significant time period, and we assume therefore that the average direction of these sites is also largely free from residual PSV.

The timing of magnetization acquisition may be determined using field tests of palaeomagnetic stability, the most common of which is the palaeomagnetic tilt test (McElhinny 1964; McFadden and Jones 1981). Unfortunately, outcrop-scale folds are rare in the Kyrenia Range and could not be palaeomagnetically sampled to allow a conventional fold test. Increases in locality mean Fisher precision parameters following application of tilt corrections to sites from the eastern range and Karpas Peninsula suggest that pre-deformational remanences are preserved in the sampled units. Data from these localities fail the Watson (1983) common mean direction test ($V_w$ = 10.7, critical value = 8.3), and are therefore statistically distinct. Differences in tilt corrected declinations and very similar tilt corrected inclinations suggest that differential vertical axis rotation has occurred between these localities, invalidating use of a standard area-wide tilt test based on full remanence vectors. Hence, we adopt an alternative, inclination-only tilt test formulation (Enkin and Watson 1996) to maximise the information incorporated into the statistical analysis. This inclination-only test is independent of the structural history and assumes that the angle between the inclination and the identified palaeohorizontal at a site remains constant during rigid body rotation. A statistically significant improvement of clustering of inclinations upon tilt correction from sites with different structural orientations implies that a pre-tilt magnetization has been identified (Enkin and Watson 1996). Data from the 11 sites from the eastern range and Karpas Peninsula combined yield the following statistics:

| | | |
|---|---|---|
| *In situ*: | $\hat{I}$ = 3.1° ± 22.9° | $k$ = 2.2 |
| Tilt-corrected | $\hat{I}$ = 35.6° ± 8.9° | $k$ = 14.6 |

where $\hat{I}$ and $k$ are the maximum likelihood estimates of the true mean inclination in degrees and the Fisher precision parameter respectively. Stepwise untilting gives a maximum $k$ value at 100% untilting (Fig. 7), suggesting that remanences were acquired before significant tectonic disruption of the sampled lavas. A parametric re-sampling implementation of the tilt test (Enkin and Watson 1996), using 1000 re-sampling trials and incorporating a circular standard deviation of 5° on the poles to palaeohorizontal surfaces, indicates an optimum untilting with 95% confidence limits close to 100% of untilting (Fig. 7). This may be interpreted as a positive result, indicating that remanences in the sampled sequences were acquired prior to deformation (Enkin and Watson 1996) and that the basic extrusive igneous rocks of the Kyrenia Range have not experienced remagnetization during tectonic evolution of the lineament.

The palaeomagnetically-sampled lavas are unconformably overlain by a polymict conglomerate of latest Eocene-early Oligocene age, which forms the base of the transgressive Bellapais (Beylerbey) Formation (Fig. 2). This conglomerate contains numerous clasts of basic-diabasic igneous rocks (McCay and Robertson 2012; Robertson et al. 2014) that were sampled at two sites (Fig. 5) in order to perform conventional palaeomagnetic conglomerate tests and provide further support for retention of original magnetizations. The conglomerates are clast-supported, to locally matrix-supported, with clasts ranging from near equidimensional to elongate (McCay 2010). Clast imbrication is locally observed (McCay and Robertson 2012) but areas without preferential clast orientation were selected for palaeomagnetic sampling. Common cobbles of relatively unaltered basalt and diabase proved to be well suited to palaeomagnetic analysis. At both sites, directions of ChRMs vary widely between individual clasts but share similar remanence characteristics and rock magnetic properties with samples from the main extrusive sites (Fig. 8). The resultant $R$ of unit vectors representing the ChRMs of individual clasts at each site were as follows:

| | |
|---|---|
| Site KR11 (Western Range): | $R$ = 1.71, n = 8 |
| Site KR24 (Karpas Peninsula): | $R$ = 3.22, n = 10 |

The corresponding critical values (below which a distribution is statistically random) for n = 8 and n = 10 are $R_0$ = 4.48 and $R_0$ = 5.03, respectively (Watson 1956). In both cases, therefore, these data constitute statistically positive palaeomagnetic conglomerate tests indicating a lack of regional-scale pervasive remagnetization of extrusive lithologies.

*Tectonic analysis*

Tectonic interpretation of palaeomagnetic data is achieved by comparing observed magnetization vectors with a reference (expected) magnetization vector, most commonly calculated from an appropriate apparent polar wander path (APWP). The Kyrenia Range is interpreted to have formed part of the northern, active continental margin of the Southern Neotethys. This ocean basin formed by the rifting of microcontinental fragments from the north-Gondwana (North African) margin during Late Triassic time (Robertson & Dixon 1984; Dercourt *et al.* 1986, 2000; Robertson 1998; Barrier & Vrielynck 2009; Robertson et al., this volume). It is appropriate, therefore, to compare the observed directions with a reference direction derived from the African APWP. A recent analysis of global APWPs was provided by Torsvik et al. (2012). Their 70 Ma (i.e. Maastrichtian) African palaeomagnetic pole ("Global APWP in South African co-ordinates") gives an associated reference direction of magnetization of Dec = 357.0°, Inc = 32.0° for sites in the Kyrenia Range (latitude = 35.5°N; longitude 34.1°E). Comparison of the tilt corrected locality mean directions of magnetization (Table 1) with this reference direction using the methodology of Butler (1992) yields rotations, *R,* of -2.2° ± 20.9° for the eastern range and -31.2° ± 12.3° for the Karpas Peninsula. The data, therefore, do not indicate any significant tectonic rotation of the eastern range and a c. 30 anticlockwise rotation of the Karpas Peninsula since the Maastrichtian. This relative rotation is consistent with the change in local strike between these localities. However, we also note that the restricted data available from the eastern range result in large uncertainties in both the locality mean direction and resulting *ΔR* confidence limit. Furthermore, as noted above the data from the western and central range segments are not interpretable.

The mean inclinations for the localities in the eastern range and the Karpas Peninsula (Table 1) are consistent with that of the reference direction, with flattening parameters (Butler 1992), *F*, of -1.1° ± 17.6° and -3.3° ± 10.4, respectively. These data suggest that the Kyrenia Range has maintained the same relative N-S position compared to stable Africa since the Maastrichtian. The palaeolatitude of the range in the Maastrichtian was $19.7°N^{+6.5°}_{-5.6°}$, as calculated from the maximum likelihood estimate of the true mean inclination derived using the inclination-only tilt test (Enkin and Watson 1996). This is comparable to the Late Cretaceous palaeolatitude of 20.6°N ± 1.8° for the spreading axis of the Troodos ophiolite, as calculated by Morris (2003) from a compilation of 100 sites of published data from the Troodos extrusive series and sheeted dyke complex. When uncertainties on the palaeolatitude constraints are considered, these data are compatible with reconstructions placing the Kyrenia Range along the northern margin of the Southern Neotethys (e.g. Robertson and Woodcock 1986), up to several hundred kilometres north of the Neotethyan spreading axis.

## Discussion and interpretation

### *Rotation of the Kyrenia Range in relation to the Troodos-Hatay microplate*

It has been hypothesised that the rotation of the Troodos-Hatay microplate was a consequence of the collision of an intra-oceanic subduction zone with the Arabian promontory of the North African continental margin (Clube et al. 1985; Clube and Robertson 1986; Robertson 1990; Morris et al. 1990; Morris 1996; Inwood et al. 2009). The Troodos and Hatay ophiolites are considered to have initially formed by spreading above a northward-dipping subduction zone within the Southern Neotethys during Late Cretaceous time (c. 90 Ma) (Fig. 9a). The palaeomagnetic evidence from the Hatay ophiolite suggests that part of the microplate rotation took place within the Southern Neotethys during the latest Cretaceous, in response to oblique subduction that preceded ophiolite emplacement (Inwood et al. 2009; Fig. 9b). The subduction zone later converged on the Arabian promontory. This resulted in the emplacement of the Hatay and Baer-Bassit ophiolites, while the Troodos ophiolite remained within the remnant Southern Neotethys further west. The subduction trench collided with the Arabian margin during latest Cretaceous time, emplacing the Hatay, Baer-Bassit and some other ophiolites (Fig. 9c). This, in turn, induced anticlockwise pivoting and thus further anticlockwise rotation of the by-then relict subduction zone. The Troodos ophiolite remained above this relict subduction zone and continued to rotate anticlockwise in the remaining Southern Neotethys until Early Eocene time (Clube et al. 1985; Clube and Robertson 1986).

Between the latest Cretaceous and the Eocene, the northern boundary of the rotated microplate should logically be located between the oceanic Troodos ophiolite and the Tauride continental margin to the north, now represented by the Kyrenia Range. Since formation, the Mesozoic-Late Miocene units of the Kyrenia Range, including the sampled basaltic extrusives, have been thrust southwards relative to the Troodos ophiolite. The Mid-Eocene thrusting could have been on the order of tens of kilometres relative to the Troodos ophiolite. In addition the latest Miocene-earliest Pliocene thrusting is likely to have added at least several kilometres to the southward displacement. The most likely present-day location of the former northern boundary of the Troodos-Hatay microplate is, therefore, beneath the deep-water Cilicia Basin between Cyprus and the Turkish mainland.

*Palaeomagnetic rotation data in relation to the structural development of the Kyrenia Range*

There is a distinct contrast between the internal consistency of palaeomagnetic data obtained from localities in the eastern parts of the Kyrenia Range compared to the tectonically uninterpretable data obtained in the western range (Table 1). This may be explained by variation in the degree of structural complexity along the range, which has variably undergone four main phases of convergence-related deformation.

The first phase involved Late Cretaceous greenschist facies metamorphism of the Lower Triassic to Cretaceous (pre-Maastrichtian) carbonate platform succession (Trypa (Tripa) Group; see Fig. 2). These older metamorphosed rocks were not palaeomagnetically sampled although their deformation and metamorphism are likely to have influenced the structural development of the younger units (e.g. by fault re-activation).

The second convergent phase involved regional-scale southward thrusting during the Mid-Eocene (Ducloz 1972; Baroz 1979; Robertson and Woodcock 1986; Robertson et al. 2014). The southward thrusting was associated with the development of locally intensive pressure solution cleavage, localised folding and c. N-S transverse faulting (Robertson and Kinnaird, this volume). The palaeomagnetically sampled Maastrichtian-Early Eocene basaltic lavas were involved in the Mid-Eocene thrusting.

The third convergent deformation phase resulted in major southward-directed thrusting and folding during latest Miocene-Early Pliocene time (Ducloz 1972; Baroz 1979; Robertson and Woodcock 1986; McCay and Robertson 2013; Robertson et al. 2014; Robertson and Kinnaird, this volume). The thrusting resulted in Late Eocene-Miocene sediments of the Mesaoria Basin to the south of the Kyrenia Range being incorporated into the thrust stack, especially in the western range. The thrust stack in the western range was specifically deformed into kilometre-scale south-verging nappe structures that have not been mapped further west in the range. In addition, the latest Miocene-Early Pliocene thrusting was accompanied by localised back-thrusting, which is well developed in the western range. It should also be noted that the Late Miocene-earliest Pliocene convergent deformation (and probably also the preceding Mid-Eocene deformation) was associated with distributed left-lateral transpression, which increased the structural complexity of some areas (McCay and Robertson, 2013; Robertson and

Kinnaird, this volume). The central range, in particular, was also extensively segmented by c. N-S transverse high-angle faults ranging from outcrop to mountain scale (Robertson and Kinnaird, this volume).

All of the palaeomagnetically sampled units experienced the latest Miocene-Early Pliocene thrusting. However, the extent and effects of the re-thrusting and folding varies strongly along the length of the range, being most marked in the western range, where the sample sites lie largely within the overturned limb of a large southward-vergent nappe, which itself includes several Eocene-age thrust sheets (Baroz 1979; Hakyemez et al. 2000; Robertson et al. 2014; Robertson and Kinnaird, this volume).

During the fourth and final phase of convergence-related deformation, the Kyrenia Range underwent strong tectonic uplift during Late Pliocene-Quaternary time (Ducloz 1972; Dreghorn 1978; Robertson and Woodcock 1986; Harrison et al. 2004; McCay and Robertson 2013; Palamakumbura et al. this volume).

The likely explanation for the inconsistency in palaeomagnetic data from the western range is that these sites experienced complex, multiple rotations during the successive Mid-Eocene and latest Miocene-earliest Pliocene phases of thrusting and folding, which cannot be restored with the available structural and palaeomagnetic information. Standard palaeomagnetic tilt corrections assign all deformation to single, net rotations around strike-parallel axes, and it is well known that this approach breaks down in areas of complex, non-coaxial, multiphase deformation and may result is substantial declination errors (MacDonald 1980). Unfortunately, sample sites in the central range were sparse due to relatively small, fragmentary exposures, and were also located close to a major thrust that bounds the southern exposure of the Kyrenia Range. Only one site carried a stable magnetization and is insufficient alone to interpret tectonically.

In the relatively structurally simple eastern Kyrenia Range and the Karpas Peninsula, tilt corrected palaeomagnetic results demonstrate a significant relative rotation between the sample sites, with minor to null rotation in the eastern range and 30° anticlockwise rotation of the Karpas Peninsula. This shows that the Kyrenia Range does not share a common 90° anticlockwise rotation history with the Troodos ophiolite to the south, which is known to have undergone a large bulk rotation (Moores and Vine 1971; Clube 1986; Clube and Robertson 1986). This rotation does not vary on the scale of the exposed ophiolite except in localised areas internal to the ophiolite, specifically associated with the Southern Troodos Transform Fault Zone (MacLeod et al. 1990), where variable rotations of small fault blocks within and adjacent to the transform are inferred (Clube 1986; Clube and Robertson 1986; Bonhommet et al. 1988; Allerton and Vine 1990; MacLeod et al. 1990; Morris et al. 1990; Cooke et al., 2014). The adjacent Hatay ophiolite in southern Turkey (Fig. 1) has also undergone a c. 90° anticlockwise rotation, similar to the Troodos ophiolite, implying that the rotated microplate was relatively large (Inwood et al. 2009), with implications for the wider region including the Kyrenia Range.

The timing of anticlockwise rotation of the Karpas Peninsula relative to the eastern range is unconstrained by the palaeomagnetic evidence and, therefore, must be considered in the context of the geological development of the Kyrenia Range. Three main options exist:

(i) Mid-Eocene: with rotation associated with southward thrusting of the Kyrenia Range as a pile of gently inclined thrust sheets. The driving force for the thrusting relates to northward subduction of the Southern Neotethys in which subduction was possibly triggered or accelerated by suturing of the Izmir-Ankara-Erzincan ocean (‘Northern Neotethys’) in central Anatolia (Robertson et al. 2014). Comparable Early-Mid Eocene southward thrusting affects the Tauride Mountains of central Anatolia (Fig. 9d). However, the thrusts retain an overall E-W trend over tens to hundreds of kilometres (MTA 2002) and there is no obvious reason why the

Eocene thrusting of the Kyrenia Range should have resulted in significant internal rotation of the range as a whole. On the other hand, detailed structural work shows that the Eocene thrusting was associated with localised westward-or northwestward-directed outcrop-scale folding, which is explained by oblique sinistral transpression (Robertson and Kinnaird, this volume). However, any resulting rotations are likely to have been on a small scale, within the thrust belt rather than affecting the lineament as a whole.

(ii) Late Eocene-Late Miocene: The Southern Neotethys in SE Turkey finally sutured during the Early Miocene (Yılmaz 1993; Robertson et al. 2007, 2015; Okay et al. 2010). A relict oceanic basin survived further west within the easternmost Mediterranean area, still capable of minor northward subduction (Fig. 9e). As a result the former accretionary margin, represented by the Mesozoic-Miocene units of the Kyrenia Range, was pinned to the east but able to pivot southwards within the relict oceanic basin. This rollback potentially took place during Late Eocene-Late Miocene, during which time deep-water siliciclastic sediments were accumulating to the south, represented by the Kythrea (Değirlenlik) Group (Weiler 1970; McCay and Robertson 2012; see Fig. 2). The sedimentary record from the south of Cyprus provides additional evidence of southward extension (Kinnaird and Robertson, 2013). However, it is more likely that the 30° anticlockwise rotation of the Karpas Peninsula was triggered by the suturing of the Southern Neotethys in southern Turkey, in which case the rotation and associated rollback took place during the Mid-Late Miocene.

(iii) Late Miocene-earliest Pliocene: This tectonic phase resulted in further southward thrusting in a setting of oblique sinistral transpression (McCay and Robertson 2013). Most of the major c. N-S trending fault zones cutting the Kyrenia Range appear to have been created during this third deformation phase, although some of these features probably date from the Mid-Eocene phase (Robertson and Kinnaird, this volume). The Late Miocene-earliest Pliocene phase of thrusting and folding can be correlated with the post-collisional suture zone tightening that affected SE Turkey, including the Misis Mountains (Robertson et al., 2004). The relative rotation of the Karpas Peninsula could therefore be a manifestation of post-collisional suture zone tightening with buckling of the Kyrenia lineament towards a relict oceanic area to the south. However, by Late Miocene-earliest Pliocene time there is no evidence that oceanic crust remained to the south (between the Troodos and the Kyrenia Range), which could have accommodated the implied southward arcuate slab rollback.

The most likely option is that the anticlockwise rotation of the Karpas Peninsula resulted from option (ii) i.e. pivoting of an unconstrained active margin, combined with rollback of the relict Southern Neotethyan subduction zone during Mid-Late Miocene Miocene (Fig. 9e). There is no obvious structural break between potentially rotated and non-rotated areas in the field. However, it should be noted that the overall arcuate trend of the Kyrenia Range is likely to have been accommodated by vertical-axis rotations involving numerous variably spaced c E-W thrusts and c. N-S steep faults. The c. N-S faults show common evidence of both sinistral and dextral strike-slip (Robertson and Kinnaird, this volume) emphasising the potential complexity of the rotation history.

Finally, the regional-scale rotation of the Troodos-Hatay microplate during latest Cretaceous-Eocene and the more localised rotation of the Karpas Peninsula can be seen as on-going effects of the collision of two different subduction zones – one oceanic (Troodos) and the other of continental margin type (Kyrenia) – with the Arabian promontory of the African continental margin. The overall tectonic process may be comparable with the well-documented development of the Aegean arc that was potentially triggered by suturing of the Southern Neotethys in southern Turkey (e.g. Le Pichon and Angelier 1979; Jolivet and Faccenna 2000). However, the inferred Neogene rollback of the Kyrenia-Cyprus arc was on a much smaller scale and less pronounced than that of the Aegean arc.

## Conclusions

1. The Kyrenia Range has a rotation history that is distinct from that of the Troodos-Hatay microplate, as now represented by the Troodos ophiolite to the south and Hatay ophiolite to the east.
2. An implication is that the northern margin of the Troodos-Hatay microplate was located between the Troodos ophiolite and the Kyrenia Range during the pre-Middle Eocene period of microplate rotation.
3. Palaeomagnetic data from the eastern segment of the Kyrenia Range (three reliable sites) and from the contiguous Karpas Peninsula (eight reliable sites) demonstrate c. 30° of relative anticlockwise rotation between these areas. This suggests that the present-day curvature of the Kyrenia Range was acquired by tectonic rotation rather than originating as a primary palaeogeographical feature.
4. In contrast the western range and the central range did not provide interpretable palaeomagnetic data. The western range has experienced strong multiphase southward thrusting and folding (Eocene and Late Miocene-earliest Pliocene), including large-scale nappe formation. The resulting complex tectonic evolution cannot be reconstructed by applying standard tilt corrections to the palaeomagnetic data.
5. The anticlockwise rotation of the Karpas Peninsula relative to the eastern range is likely to be linked to suturing of the Southern Neotethys during the Mid-Late Miocene. The Arabian continental indentor sutured the Tauride accretionary margin with the Anatolian microcontinent (~Eurasian plate) in the east, while a relict subduction zone was able to migrate (rollback) southwards, inducing the observed curvature.

## Acknowledgements

Mustafa Alkaravli kindly made available the logistical support of the Geology and Minerals Department during this work. Mehmet Necdet helped with the logistics and with the discussion of the geology. We thank Gillian McCay and Salih Ersangil for assistance in the field and Costas Xenophontos for discussions of the regional geology in the field. An award from the Nuffield Science Bursaries for Undergraduate Research supported eight weeks of laboratory analysis by Emma Hodgson at Plymouth University. Constructive reviews by Maude Meijers, Jenny Inwood and Mualla Cengiz Cinku enabled us to significantly improve the paper.

## References

Aksu AE, Hall J, Yaltıra C (2009) Miocene–Recent evolution of Anaximander Mountains and Finike Basin at the junction of Hellenic and Cyprus Arcs, eastern Mediterranean, Marine Geology 258: 24–47

Allerton S, Vine FJ (1990) Palaeomagnetic and structural studies of the southeastern part of the Troodos complex. In: Malpas J, Moores EM, Panayiotou A, Xenophontos C. (eds) Ophiolites: Oceanic Crustal Analogues.

Cyprus Geol Surv Dept pp. 99–111

Bağcı U, Parlak O (2009) Petrology of the Tekirova (Antalya) ophiolite (Southern Turkey): Evidence for diverse magma generations and their tectonic implications during Neotethyan-subduction. Int J Earth Sciences 98: 387–405

Baroz F (1979) Etude géologique dans le Pentadaktylos et la Mesaoria (Chypre Septentrionale), Docteur d' État thesis, Université de Nancy

Baroz F (1980) Volcanism and continent-island arc collision in the Pentadaktylos range, Cyprus. In: Panayiotou A (ed) Ophiolites Proc Int Symp Nicosia, Cyprus, pp. 73-75

Barrier E, Vrielynck B. (eds) (2009) Palaeotectonic Maps of the Middle East. Paris: Middle East Basins Evolution Programme

Bonhommet N, Roperch P, Calza F (1988) Paleomagnetic arguments for block rotations along the Arakapas Fault (Cyprus). Geology 16: 422–425

Butler RF (1992) Paleomagnetism: magnetic domains to geologic terranes. Blackwell Scientific Publications, Oxford, 319 pp

Calon TJ, Aksu AE, Hall J (2005) The Oligocene-Recent evolution of the Mesaoria Basin (Cyprus) and its western marine extension, Eastern Mediterranean. Marine Geology 221: 95-120

Clube TMM, Creer, KM, Robertson, AHF (1985) The palaeorotation of the Troodos microplate. Nature 317: 522-525

Clube TMM, Robertson AHF (1986) The palaeorotation of the Troodos microplate, Cyprus in the Late Mesozoic-Early Tertiary plate tectonic framework of the Eastern Mediterranean: Surveys in Geophysics 8: 375-437

Clube TMM (1986) The palaeorotation of the Troodos microplate. Unpubl. PhD Thesis, Univ. Edinburgh 275pp.

Cooke AJ, Masson, LP, Robertson, AHF (2014) Construction of a sheeted dyke complex: evidence from the northern margin of the Troodos Ophiolite and its southern margin adjacent to the Arakapas Fault Zone. Ofioliti 39:1-30

Deenen MHL, Langereis CG, van Hinsbergen DJJ, Biggin AJ (2011) Geomagnetic secular variation and the statistics of palaeomagnetic directions. Geophys J Internat 186:509-520

Dercourt J, Gaetani M, Vrielynck B, Barrier E, Biju-Duval B, Brunet MF, Cadet JP, Crasquin S, Sandulescu M (2000) Peri-Tethys Palaeogeographical Atlas 2000. Paris: Commission de la Carte Géologique du Monde/Commission for the Geologic Map of the World

Dercourt J, Zonenshain L-P, Ricou LE, Kazmin VG, Le Pichon X, Knipper AL, Grandjacquet C, Sbortshikov IM, Geyssant J, Lepvrier C, Pechiersky DH, Boulin J, Sibuet JC, Savostin LA, Sorokhtin O, Westphal M, Bazhenov ML, Lauer JP, Bijuduval, B (1986) Geological evolution of the Tethys belt from the Atlantic to the Pamirs since the Lias. Tectonophysics 123: 241–315

Dreghorn W (1978) Landforms of the Girne Range, Northern Cyprus. Miner. Res. Explor. Inst. (MTA), Turkey 172 pp.

Ducloz C (1972) The geology of the Bellapais-Kyrthrea area of the central Kyrenia Range. Cyprus Geol Surv Bull 6. Geol Surv Depart, Nicosia, Cyprus

Dunlop DJ, Özdemir Ö (1997) Rock Magnetism: Fundamentals and Frontiers. Cambridge University Press

Enkin R.J, Watson GS (1996) Statistical analysis of palaeomagnetic inclination data. Geophysical Journal International 126:495-504

Fisher RA (1953) Dispersion on a sphere. Proc Roy Soc London A217: 295–305

Glover C, Robertson AHF (1998) Neogene intersection of the Aegean and Cyprus arcs: extensional and strike-slip faulting in the Isparta Angle, SW Turkey. Tectonophysics 298: 103–132

Gradstein FM, Ogg JG, Schmitz MD, Ogg GM (2012) The Geologic Time Scale 2012. (Oxford, UK.), Elsevier, ISBN-9780444594259

Hakyemez Y, Turhan N, Sönmez, İ, Sümengen M (2000) Kuzey Kıbrıs Türk Cumhuriyeti' nin Jeolojisi, MTA. Genel Müdürlüğü Jeoloji Etütleri Diaresi, Ankara: 44 pp.

Harrison R W, Newell WL, Batihanli H, Panayides I, McGeehin JP, Mahan S A, Ozhur A, Tsiolakis E, Necdet M (2004) Tectonic framework and Late Cenozoic tectonic history of the northern part of Cyprus: implications for earthquake hazards and regional tectonics. J Asian Earth Sci 23: 191-210

Hodgson E, Morris A, Anderson MW, Robertson AHF (2010) First palaeomagnetic results from the Kyrenia Range terrane of northern Cyprus and their implication for the regional plate tectonic evolution of the eastern Mediterranean. Geophys Res. Abstrs 12: 6449, European Geosciences Union General Assembly, Vienna

Huang K (2008) Geological studies of igneous rocks and their relationships along the Kyrenia Range, Northern Cyprus. Unpub MPhil thesis, Univ Hong Kong 187pp.

Huang K, Malpas J, Xenophontos C (2007) Geological studies of igneous rocks and their relationships along the Kyrenia Range. In: Moumani K, Shawabkeh K, Al-Malabeh, A, Abdelghafoor M (eds) Absts. 6th Internat Congr Eastern Mediterranean Geology 2–5 April 2007, Amman, Jordan, p 53

Inwood J, Morris A, Anderson MW, Robertson AHF (2009) Neotethyan intraoceanic microplate rotation and variations in spreading axis orientation: palaeomagnetic evidence from the Hatay ophiolite (southern Turkey).

Earth Planet Sci Letts 280: 105-117

Jolivet L, Faccenna C (2000) Mediterranean extension and the Africa-Eurasia collision. Tectonics 19: 1095-1106

Kelling G, Gokcen SL, Floyd PA, Gökçen N (1987) Neogene tectonics and plate convergence in the eastern Mediterranean: new data from southern Turkey. Geology 15: 425–429

Kempler D, Garfunkel Z (1994) Structures and kinematics in the northeastern Mediterranean: a study of an irregular plate boundary. Tectonophysics 234:19-32

Kinnaird TC, Robertson AHF (2013) Neogene tectonics and basin architecture of the southern margin of the Mesaoria Basin: implications for the southern margin of the Anatolian plate. In: Robertson AHF, Parlak O, Ünlügenç Ü. (eds), Geological Development of Anatolia and the Easternmost Mediterranean region. Geol Soc London, Spec Publ 372: 585–614

Kirschvink JL (1980) The least-squares line and plane and the analysis of palaeomagnetic data. Geophys J Royal Astromomical Soc 62:699–718

Le Pichon X, Angelier J (1979) The Aegean Arc and trench system: a key to the neotectonic evolution of the eastern Mediterranean area, Tectonophysics 60: 1-42

MacDonald WD (1980) Net tectonic rotation, apparent tectonic rotation, and the structural tilt correction in palaeomagnetic studies. J. Geophys. Res., 85: 3659-3669

MacLeod CJ, Allerton S, Gass IG, Xenophontos C (1990) Structure of a fossil ridge-transform intersection in the Troodos ophiolite. Nature 348: 717–720

McCay G, Robertson AHF (2012) Sedimentology and provenance of Upper Eocene-Upper Miocene clastic sediments of the Girne (Kyrenia) Range, northern Cyprus: A case history of sedimentation related to progressive and diachronous continental collision. Sedimentary Geology 265: 30-55

McCay G, Robertson AHF (2013) Upper Miocene–Pleistocene deformation of the Girne (Kyrenia) Range and Dar Dere (Ovgos) lineaments, northern Cyprus: role in collision and tectonic escape in the easternmost Mediterranean region. In: Robertson AHF, Parlak O, Ünlügenç Ü. (eds) Geological Development of Anatolia Continent and the Easternmost Mediterranean Region. Geol Soc London, Spec Publ 254: 421-446

McCay G, Robertson AHF, Kroon D, Raffi, I, Ellam RM. Necdet M (2013) Stratigraphy of Cretaceous to Lower Pliocene sediments in the northern part of Cyprus based on comparative 87Sr/86Sr isotopic nannofossil and planktonic foraminiferal dating. Geol Mag150: 333-359

McCay G (2010) Tectonic-sedimentary evolution of the (Kyrenia) Girne Range and the Mesarya (Meraoria) Basin, North Cyprus. Unpub Univ Edinburgh PhD thesis

McElhinny MW (1964) Statistical significance of the fold test in palaeomagnetism. Geophys J Royal

Astronomical Soc 8:338–340

McFadden PL, Jones DL (1981) The fold test in palaeomagnetism. Geophys J Royal Astronomical Soc 67:53–58

Moores EM, Vine FJ (1971) The Troodos Massif, Cyprus and other ophiolites as oceanic crust: evaluations and implications. Phil Trans R Soc A 268: 433-466

Morris A (1996) A review of palaeomagnetic research in the Troodos ophiolite, Cyprus. In: Morris A, Tarling DH (eds.) Palaeomagnetism and Tectonics of the Mediterranean Region. Geol. Soc. London Spec. Publ 105:311-324

Morris A (2003) The Late Cretaceous palaeolatitude of the Neotethyan spreading axis in the eastern Mediterranean region. Tectonophysics 377: 157-178

Morris A, Anderson MW, Inwood J, Robertson AHF (2006) Palaeomagnetic insights into the evolution of Neotethyan oceanic crust in the eastern Mediterranean. In: Robertson AHF, Mountrakis D. (Eds) Tectonic Development of the Eastern Mediterranean Region, Geol Soc London Spec Publ 260: 351-372

Morris A, Anderson MW, Robertson AHF (1998) Multiple tectonic rotations and transform tectonism in an intra-oceanic suture zone, SW Cyprus. Tectonophysics 299: 229-253

Morris A, Creer KM, Robertson AHF (1990) Palaeomagnetic evidence for clockwise tectonic rotations related to dextral shear along the Southern Troodos Transform Fault, Cyprus. Earth Planet Sci Letts 99: 250-262

Morris A, Tait JA (2003) Geodynamic applications of palaeomagnetism - introduction. Tectonophysics, 377: 1-5

MTA 2002. Geological Map of Turkey 1:500,000, Maden Tektik ve Arama Genel Müdürlüğü. (General Directorate of Mineral Research and Exploration), MTA, Ankara

Musaka SB, Ludden JN (1987) Uranium-lead ages of plagiogranites from the Troodos ophiolite, Cyprus, and their tectonic significance. Geology 15: 825–828

Okay Aİ, Zattin M, Cavazza W (2010) Apatite fission-track data for the Miocene Arabia-Eurasia collision. Geology, 38: 35-38

Palamakumbura RN, Robertson AHF, Kinnaird, T, Sanderson, DCW Using sedimentology and luminescence to differentiate between tectonic and eustatic influences on the Quaternary terraces of northern Cyprus. This volume In J earth Science, this volume (accepted manuscript).

Poisson A (1977) Récherches Géologiques dans les Taurides Occidentales, Turquie. Doctoral Thesis, Univ Paris-Sud, Orsay, France

Robertson AHF (1990) Tectonic evolution of Cyprus. In: Malpas J, Moore E M, Panayiotou A, Xenophontos C. (eds) Ophiolites: Oceanic crustal analogues: Proc Internat Symp. Cyprus Geol Surv Dept, Nicosia, Cyprus 235–252

Robertson AHF (1998) Mesozoic-Tertiary tectonic evolution of the easternmost Mediterranean area: integration of marine and land evidence. Proc. ODP Ocean, Science Results 160: 723-782

Robertson AHF, Boulton SJ, Taslı K, Yıldırım N, İnan N, Yıldız A, Parlak O Late Cretaceous-Miocene sedimentary development of the Arabian continental margin in SE Turkey (Adıyaman Region): implications for regional palaeogeography and the closure history of Southern Neotethys. J Asian Earth Sci (accepted manuscript).

Robertson AHF, Dixon JE (1984) Introduction: Aspects of the Geological Evolution of the Eastern Mediterranean. In Dixon JE, Robertson AHF (eds) The Geological Evolution of the Eastern Mediterranean, Geol Soc London, Spec Publ 17: 1–74

Robertson AHF and Kinnaird TC Structural development of the Central Kyrenia Range (north Cyprus) in its regional setting in the eastern Mediterranean, Internat J Earth Science, under revision

Robertson AHF, McCay GA, Taslı K, Yıldız, A (2014) Eocene development of the northerly active continental margin of the Southern Neotethys in the Kyrenia Range, north Cyprus, Geol. Mag. 151: 692–731

Robertson AHF, Parlak O, Yıldırım N, Dumitrica P, Taslı K Late Triassic rifting and Jurassic-Cretaceous passive margin development of the Southern Neotethys: evidence from the Adıyaman area, SE Turkey. Int J Earth Sci., this volume (resubmitted)

Robertson AHF, Parlak O, Ünlügenç U., İnan N, Taslı K, Ustaömer, T (2007) Tectonic evolution of the South Tethyan ocean: evidence from the Eastern Taurus Mountains (Elazığ region, SE Turkey). In: Ries AC, Butler RWH, Graham RH (Eds) Deformation of the Continental crust: the Legacy of Mike Coward. Geol. Soc. London Spec Publ 272: 231-270

Robertson AHF, Poisson A, Akıncı (2003) Developments in research concerning Mesozoic–Tertiary Tethys and neotectonics in the Isparta Angle, SW Turkey. Geological Journal 38:195–234

Robertson AHF, Taslı K, İnan N (2012) Evidence from the Kyrenia Range, Cyprus, of the northerly active margin of the Southern Neotethys during Late Cretaceous–Early Cenozoic time. Geol Mag 149: 264-2.

Robertson AHF, Unlügenç ÜC, İnan N, Taşli, K (2004) The Misis–Andırın Complex: a Mid-Tertiary melange related to late-stage subduction of the Southern Neotethys in S Turkey. J Asian Earth Sci 22: 413-453

Robertson AHF, Woodcock NH (1986) The role of the Kyrenia Range lineament, Cyprus, in the geological evolution of the eastern Mediterranean area. Phil Trans R Soc London (A). In: Reading HG, Watterson J, White SH (eds). Major Crustal Lineaments and Their Influence on the Geological History of Continental Lithosphere pp.141-177

Robertson AHF, Woodcock NH (1982) Sedimentary history of the south-western segment of the Mesozoic-Tertiary Antalya continental margin, south-western Turkey. Eclog Geol Helv 75: 517-562

Robertson AHF, Xenophontos C (1993) Development of concepts concerning the Troodos ophiolite and adjacent units in Cyprus. In: Prichard HM, Alabaster T, Harris NBW, Neary CR. (Eds) Magmatic Processes and Plate Tectonics. Geol Soc London, Spec Publ 76: 85-119

Torsvik TH, Van der Voo R, Preeden U, Mac Niocaill C, Steinberger B, Doubrovine PV, van Hinsbergen DJJ, Domeier M, Gaina C, Tohver E, Meert JG, McCausland PJA, Cocks LRM (2012) Phanerozoic polar wander, palaeogeography and dynamics. Earth-Science Rev 114:325–368

Vidal N, Alvarez-Marron J, Klaeschen D (2000) The structure of the Africa-Anatolia plate boundary in the eastern Mediterranean. Tectonics 19: 723-739

Watson GS (1956) A test for randomness of directions. Mon. Not. Roy. Astron. Soc. Geophys. Supp. 7: 160–161

Watson G (1983) Large sample theory of the Langevin distributions. J. Stat. Plann. Inference 8: 245–256

Weiler Y (1970) Mode of occurrence of pelites in the Kythrea Flysch Basin (Cyprus) J Sed Petrol 40: 1255-1261

Xu W, Peacor DR, Dollase WA, Van der Voo R, Beaubouef R (1997) Transformation of titanomagnetite to titanomaghemite: a slow, two-step, oxidation-ordering process in MORB. Amer Mineral 82: 1101-1110

Yılmaz Y (1993) New evidence and model on the evolution of the southeast Anatolian orogen. Geol Soc America Bull 105: 251-271

Zitter TAC, Woodside JM., Mascle J (2003) The Anaximander Mountains: a clue to the tectonics of southwest Anatolia. Geological Journal 38: 375–394

**Figure captions**

Fig. 1. Outline geological map and representative cross-section of the main part of the Kyrenia Range showing the locations of the palaeomagnetic sampling sites. Red stars/orange circles = sampling sites generating interpretable/uninterpretable data, respectively. Inset: outline tectonic map of the easternmost Mediterranean region showing the distribution of Late Cretaceous ophiolites and suture zones. Red box indicates area of main map. Modified from Robertson et al. (2012).

Fig. 2. Partial stratigraphy of the Kyrenia Range including the palaeomagnetically sampled basaltic rocks of latest Cretaceous (Maastrichtian) to Mid-Eocene age (the Late Triassic-Jurassic carbonate platform rocks at the base of the succession are omitted). Simplified from Robertson et al. (2012). The timescale of Gradstein et al. (2012) was used to correlate the numerical radiometric ages with the time scale.

Fig. 3. Field photographs illustrating the local geology of sampled units in the Kyrenia Range of northern Cyprus. (a) Maastrichtian basaltic lavas overlain by pelagic carbonates within the Malounda Formation at site KR01 in the eastern range; (b) elongate, undeformed basaltic pillow lavas at site KR20 in the Karpas Peninsula showing

consistent and uniform orientation; (c) exposed cross-section through an elongate tube in undeformed pillow lavas in the Karpas Peninsula with amygdales concentrated in the centre (site KR19, located 60 m to the SE of the village of Platanisso/Balalan); (d) basaltic sheet-flow overlying pillow lavas in the Karpas Peninsula, with intervening pink interlava pelagic sediment providing palaeohorizontal control (site KR21, located c. 400 m SSE of the village of Platanisso/Balalan); (e) conglomerates of the Bellapais Formation (sampled at site KR11) transgressively overlying basaltic pillow lavas, near Vasileia (Karsıyaka); and (f) detail of matrix-supported conglomerates of the Bellapais Formation, sampled at site KR24 (600 m W of the village of Platanisso/Balalan), showing well-rounded clasts of basalt similar to the underlying Maastrichtian basalts sampled at other sites in the Karpas Peninsula.

Fig. 4. Isothermal remanent magnetization acquisition curves for basaltic lavas of the Kyrenia Range of northern Cyprus, showing saturation by 300 mT consistent with remanence carried by low coercivity magnetite. Blue histograms show rate of change of IRM acquisition, representing the associated coercivity spectra. Bottom right hand panel shows an example of the variation of low field magnetic susceptibility with temperature (see text for explanation).

Fig. 5. Examples of alternating field (AF) and thermal demagnetization behavior of samples of Maastrichtian basaltic lavas of the Kyrenia Range of northern Cyprus. Note the presence of clear, linear characteristic remanence components following removal of minor secondary components by low AF and thermal treatments. Solid circles, projection on to the horizontal plane; open circles, projection on to the vertical N–S plane.

Fig. 6. Equal area stereographic projections showing mean directions of magnetization for sites in the eastern Kyrenia Range and the Karpas Peninsula that yielded tectonically interpretable data. Left hand projections: *in situ* coordinates; right hand projections: data after application of standard tilt corrections. Solid/open symbols are projections on to the lower/upper hemispheres respectively; ellipses = projections of $\alpha_{95}$ cones of confidence around site mean remanence directions; green star = present day, geocentric axial dipole field direction; red star = reference direction derived from the African apparent polar wander path of Torsvik et al. (2012).

Fig. 7. Variation in the Fisher precision parameter with progressive untilting of sampled sites in the eastern Kyrenia Range and Karpas Peninsula (solid line), indicating a positive inclination-only tilt test with a maximum precision parameter at 100% untilting (Enkin and Watson 1996). Histogram shows the results of a parametric re-sampling implementation of the tilt test (Enkin and Watson 1996), using 1000 re-sampling trials and incorporating a circular standard deviation of 5° on the poles to palaeohorizontal surfaces.

Fig. 8. Thermal and alternating field demagnetization behavior of basaltic clasts within conglomerates of the Bellapais Formation, together with equal area stereographic projections showing the distributions of remanence directions in individual clasts sampled at sites KR11 and KR24. On demagnetization plots, solid circles = projection on to the horizontal plane, open circles = projection on to the vertical E–W plane. On stereographic projections, solid/open symbols are projections on to the lower/upper hemispheres respectively. Ellipses = maximum angular deviations associated with ChRM directions of individual clasts, found using principal

component analysis.

Fig. 9. Proposed schematic tectonic model (not to scale) to explain phases of rotation in the eastern Mediterranean Tethys. (a) Late Cretaceous sea-floor spreading-related, local-scale clockwise rotations along the South Troodos Transform Fault Zone (e.g. Bonhommet et al., 1988; Allerton and Vine, 1990; Morris et al., 1990); (b) and (c) Late Cretaceous, intraoceanic anticlockwise rotation of the Troodos-Hatay microplate and emplacement-related rotation of the Hatay ophiolite (see Inwood et al., 2009); and (e) Mid-Late Miocene anticlockwise rotation of the Karpas Peninsula relative to the eastern Kyrenia Range (this paper). Blue circular arrows = inferred senses of tectonic rotation; black arrows = regional convergence direction; blue = oceanic crust; yellow continental crust; Ky = Kyrenia Range; Tr = Troodos; H = Hatay; E = Eratosthenes Seamount.

**Table 1. Palaeomagnetic data from the Kyrenia Range**

| Site | Description | Age | n | In situ Dec | In situ Inc | Tilt corrected Dec | Tilt corrected Inc | k | $\alpha_{95}$ | Orientation (D/DD) | UTM WGS84 |
|---|---|---|---|---|---|---|---|---|---|---|---|
| **Western (tectonically uninterpretable due to structural complexity):** | | | | | | | | | | | |
| KR12 | Basaltic pillow lavas | Maastrichtian | 7 | 281.5 | -18.8 | 230.3 | 66.9 | 174.8 | 4.6 | 76/305 O/T | 36S 510366E, 3910725N |
| KR14 | Basaltic pillow lavas | Maastrichtian | 9 | 259.2 | -20.6 | 230.3 | 45.9 | 147.1 | 4.3 | 76/305 O/T | 36S 510366E, 3910725N |
| KR15 | Basaltic pillow lavas | Maastrichtian | 7 | 82.1 | 47.8 | 302.2 | 56.8 | 26.3 | 12 | 72/280 | 36S 510868E, 3910074N |
| KR16 | Basaltic pillow lavas | Maastrichtian | 9 | 98.5 | -57 | 96.8 | 47.5 | 45.4 | 7.7 | 75/090 O/T | 36S 511181E, 3909190N |
| **Central Range (tectonically uninterpretable due to structural complexity):** | | | | | | | | | | | |
| KR28 | Basaltic pillow lavas | Eocene | 7 | 326.7 | 44 | 336.7 | 1 | 107.6 | 5.8 | 48/000 | 36S 541376E, 3903046N |
| **Eastern Range (Malounda & Ayios Nikolaos):** | | | | | | | | | | | |
| KR01 | Basaltic massive lavas | Maastrichtian | 7 | 3.1 | 59.5 | 358.8 | 44.8 | 136.3 | 5.2 | 15/348 | 36S 563060E, 3910758N |
| KR03 | Basaltic pillow lavas | Maastrichtian | 7 | 12 | -43.2 | 183 | -24.6 | 102.9 | 6 | 68/187 O/T | 36S 558067E, 3909599N |
| KR04 | Basaltic pillow lavas | Maastrichtian | 7 | 319.1 | -41.8 | 162.9 | -29 | 141.6 | 5.1 | 72/152 O/T | 36S 557820E, 3909567N |
| | | | *N* = 3 | 154.7 | 68.9 | - | - | 3.2 | 85.5 | | |
| | | | *N* = 3 | - | - | 354.8 | 33.1 | 33.7 | 21.6 | | |
| **Karpas Peninsula (Platanisso):** | | | | | | | | | | | |
| KR17 | Basaltic pillow lavas | Maastrichtian | 10 | 319.5 | 4.5 | 317.9 | 46.4 | 288.7 | 2.8 | 42/143 | 36S 600408E, 3926759N |
| KR18 | Basaltic pillow lavas | Maastrichtian | 6 | 320.1 | -8.7 | 319.6 | 33.2 | 30.1 | 12.4 | 42/143 | 36S 600232E, 3926815N |
| KR19 | Basaltic pillow lavas | Maastrichtian | 11 | 319.1 | 11.8 | 318 | 63.8 | 444.8 | 2.2 | 52/140 | 36S 600693E, 3926874N |
| KR21 | Basaltic sheet flow | Maastrichtian | 6 | 324.8 | -11.5 | 326.7 | 20.5 | 101.6 | 6.7 | 39/110 | 36S 601037E, 3926970N |
| KR22 | Basaltic pillow lavas | Maastrichtian | 10 | 326.1 | -18.4 | 326.9 | 21.5 | 241.4 | 3.1 | 47/113 | 36S 601083E, 3926963N |
| KR23 | Basaltic pillow lavas | Maastrichtian | 6 | 309.9 | 1.4 | 311.6 | 39.1 | 251.1 | 4.2 | 38/124 | 36S 601168E, 3927007N |
| KR25 | Basaltic pillow lavas | Maastrichtian | 7 | 177.7 | 68.9 | 332 | 37.9 | 84.5 | 6.6 | 72/340 | 36S 599799E, 3927797N |
| KR26 | Basaltic pillow lavas | Maastrichtian | 8 | 225.7 | 77.7 | 345 | 17.6 | 23 | 11.7 | 80/355 | 36S 600304E, 3927808N |
| | | | *N* = 8 | 315.4 | 15.5 | - | - | 3.2 | 37.2 | | |
| | | | *N* = 8 | - | - | 325.8 | 35.3 | 21.1 | 12.4 | | |
| **Conglomerate test sites:** | | | | | | | | | | | |
| KR11 | Bellapais Formation, Vasileia | Latest Eocene to Early Oligocene | 8 | no site mean direction possible | | | | | | | 36S 506455E, 3910696N |
| KR24 | Bellapais Formation, Platanisso | Latest Eocene to Early Oligocene | 10 | no site mean direction possible | | | | | | | 36S 599419E, 3926518N |

n = number of samples; N = number of sites; Dec = mean declination; Inc = mean inclination; k = Fisher precision parameter; $\alpha_{95}$ = 95% cone of confidence around Fisher mean; D/DD = dip/dip direction
O/T = overturned

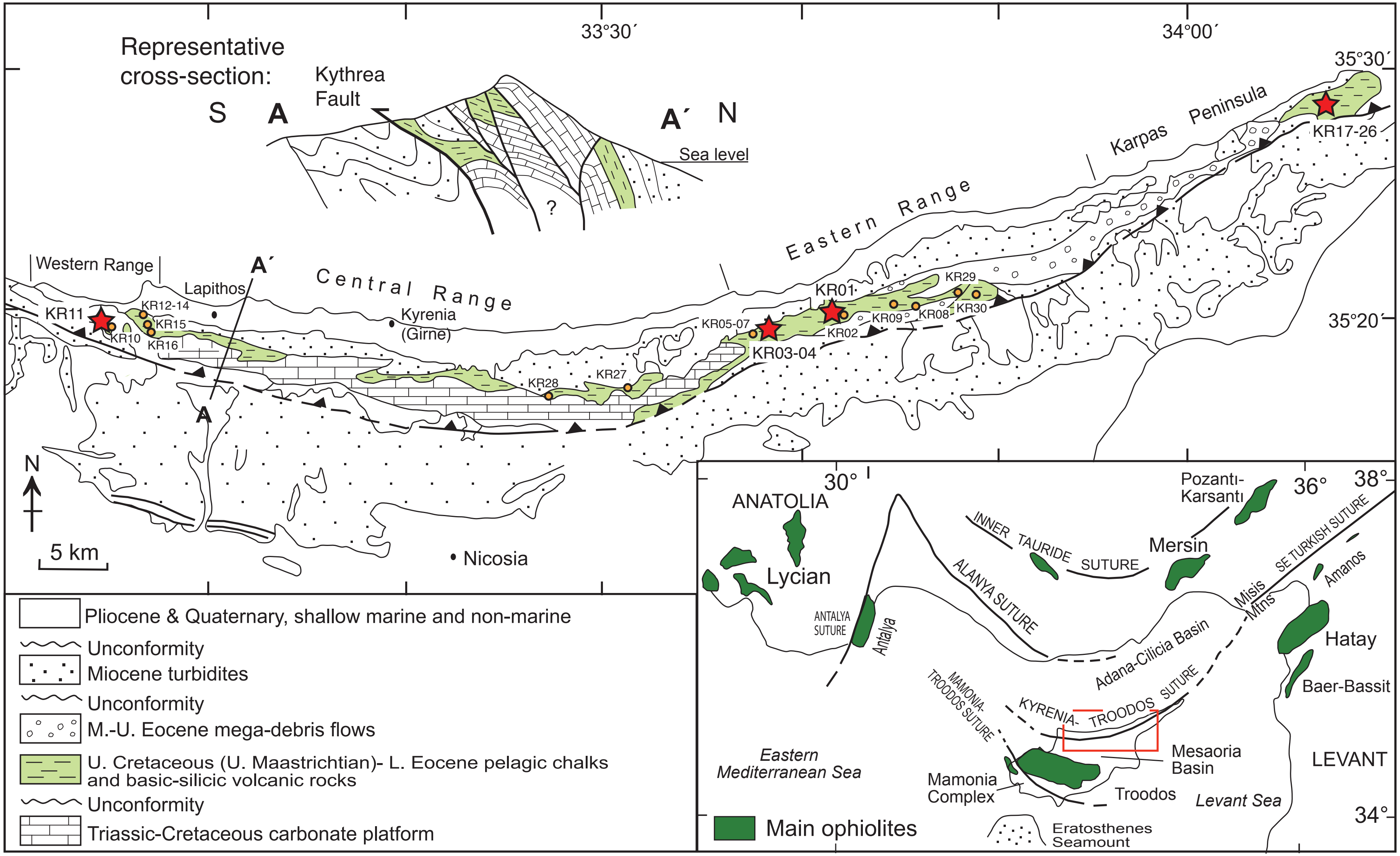
Representative cross-section:
Kythrea Fault
S
A
A´
N
Sea level
?
33°30´
34°00´
35°30´
35°20´
Karpas Peninsula
Eastern Range
Central Range
Western Range
Lapithos
Kyrenia (Girne)
Nicosia
KR11
KR12-14
KR15
KR10
KR16
KR28
KR27
KR05-07
KR03-04
KR01
KR02
KR09
KR08
KR29
KR30
KR17-26
N
5 km
Pliocene & Quaternary, shallow marine and non-marine
Unconformity
Miocene turbidites
Unconformity
M.-U. Eocene mega-debris flows
U. Cretaceous (U. Maastrichtian)- L. Eocene pelagic chalks and basic-silicic volcanic rocks
Unconformity
Triassic-Cretaceous carbonate platform
30°
36°
38°
34°
ANATOLIA
Lycian
Pozantı-Karsantı
INNER TAURIDE SUTURE
Mersin
ALANYA SUTURE
ANTALYA SUTURE
Antalya
SE TURKISH SUTURE
Amanos
Misis Mtns
Adana-Cilicia Basin
Hatay
Baer-Bassit
MAMONIA-TROODOS SUTURE
KYRENIA-TROODOS SUTURE
Mesaoria Basin
Eastern Mediterranean Sea
Mamonia Complex
Troodos
Levant Sea
LEVANT
Main ophiolites
Eratosthenes Seamount

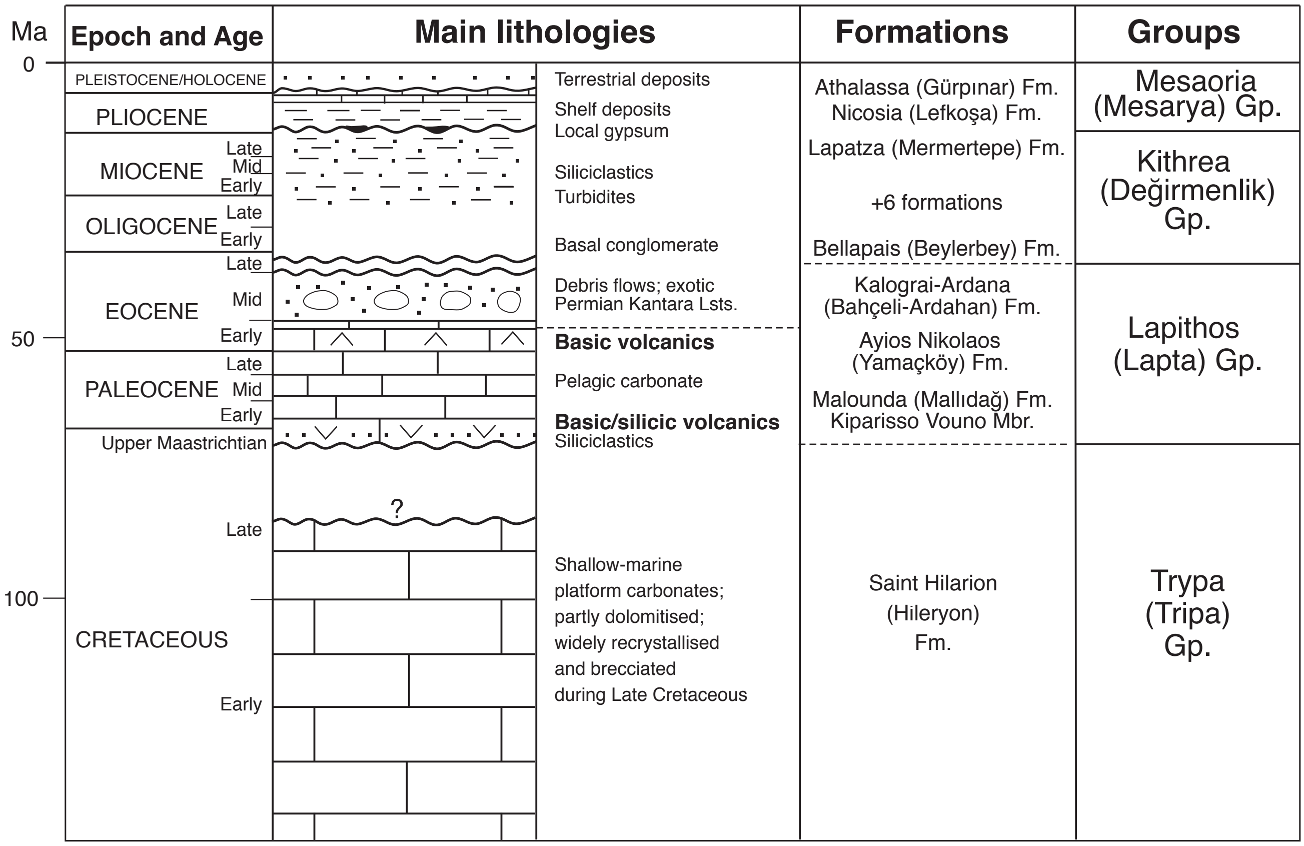
Ma
0
50
100
Epoch and Age
Main lithologies
Formations
Groups
PLEISTOCENE/HOLOCENE
PLIOCENE
MIOCENE
Late
Mid
Early
OLIGOCENE
Late
Early
EOCENE
Late
Mid
Early
PALEOCENE
Late
Mid
Early
Upper Maastrichtian
CRETACEOUS
Late
Early
?
Terrestrial deposits
Shelf deposits
Local gypsum
Siliciclastics
Turbidites
Basal conglomerate
Debris flows; exotic
Permian Kantara Lsts.
Basic volcanics
Pelagic carbonate
Basic/silicic volcanics
Siliciclastics
Shallow-marine
platform carbonates;
partly dolomitised;
widely recrystallised
and brecciated
during Late Cretaceous
Athalassa (Gürpınar) Fm.
Nicosia (Lefkoşa) Fm.
Lapatza (Mermertepe) Fm.
+6 formations
Bellapais (Beylerbey) Fm.
Kalograi-Ardana
(Bahçeli-Ardahan) Fm.
Ayios Nikolaos
(Yamaçköy) Fm.
Malounda (Mallıdağ) Fm.
Kiparisso Vouno Mbr.
Saint Hilarion
(Hileryon)
Fm.
Mesaoria
(Mesarya) Gp.
Kithrea
(Değirmenlik)
Gp.
Lapithos
(Lapta) Gp.
Trypa
(Tripa)
Gp.

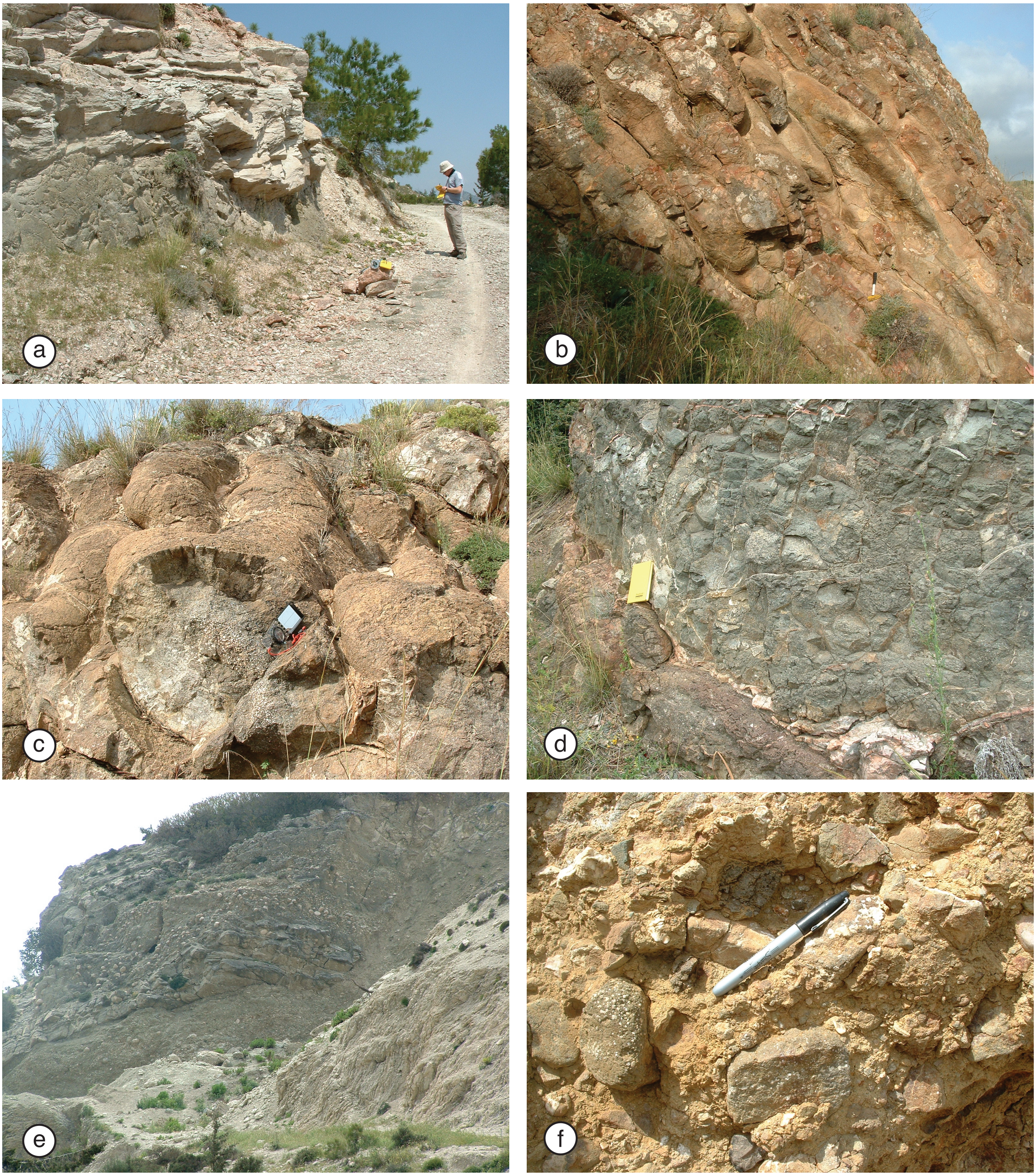
a
b
c
d
e
f

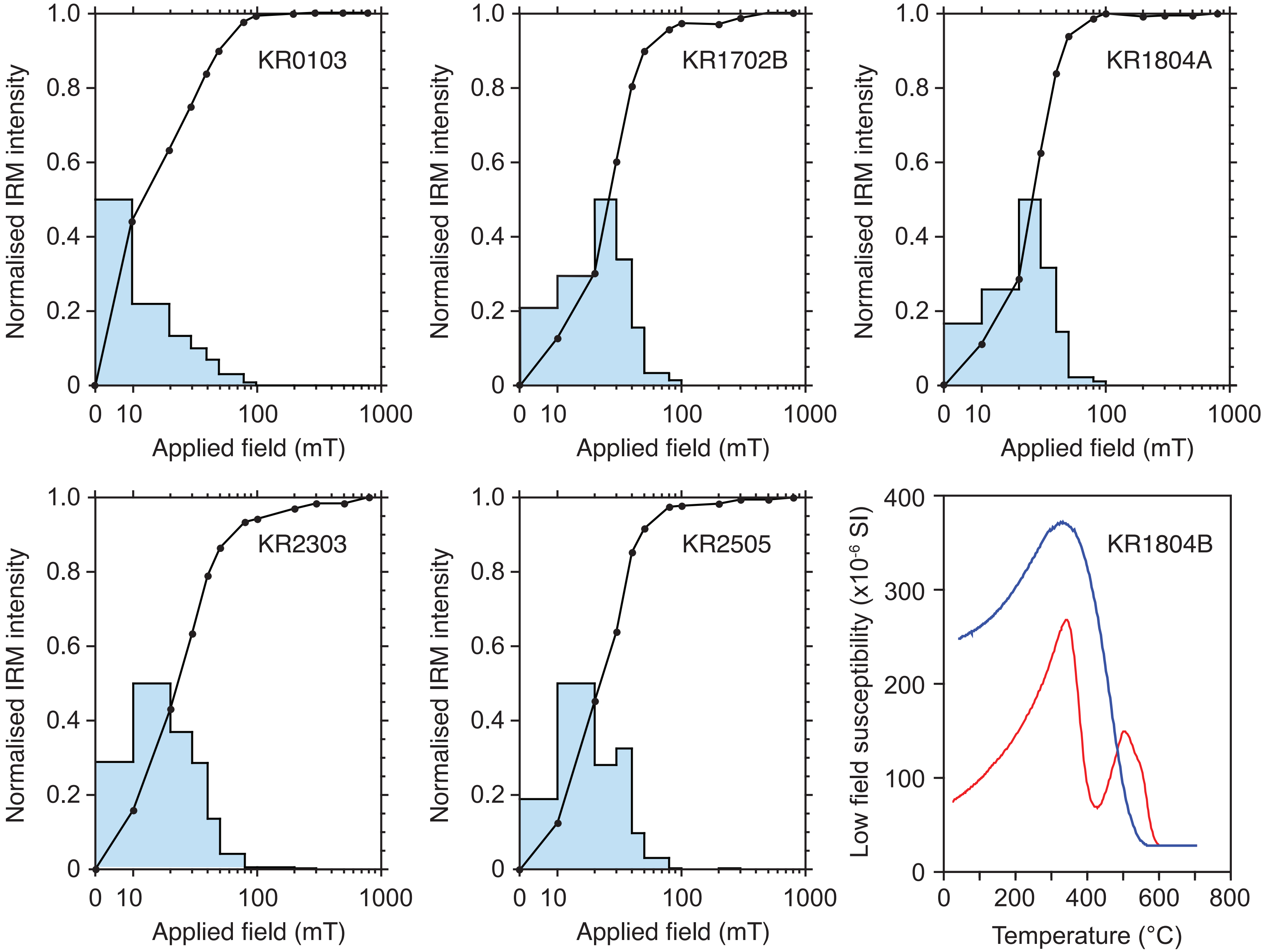

KR0103
KR1702B
KR1804A
KR2303
KR2505
KR1804B
Normalised IRM intensity
Applied field (mT)
Low field susceptibility (x10⁻⁶ SI)
Temperature (°C)

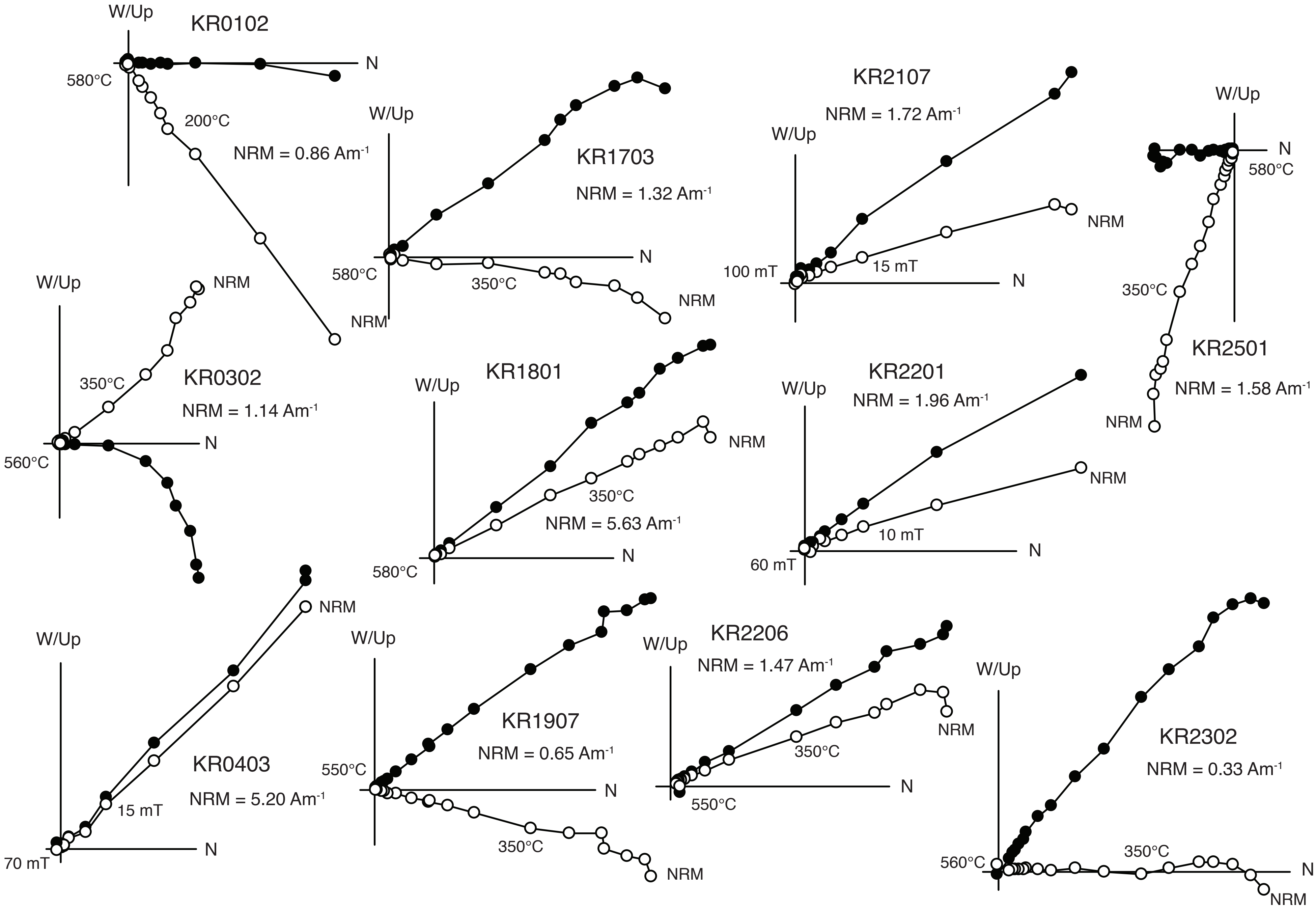
KR0102
W/Up
N
580°C
200°C
NRM = 0.86 Am-1
KR1703
W/Up
N
580°C
350°C
NRM
NRM = 1.32 Am-1
KR2107
NRM = 1.72 Am-1
W/Up
N
100 mT
15 mT
NRM
KR2501
W/Up
N
580°C
350°C
NRM
NRM = 1.58 Am-1
KR0302
W/Up
N
560°C
350°C
NRM
NRM = 1.14 Am-1
KR1801
W/Up
N
580°C
350°C
NRM
NRM = 5.63 Am-1
KR2201
NRM = 1.96 Am-1
W/Up
N
60 mT
10 mT
NRM
KR0403
W/Up
N
70 mT
15 mT
NRM
NRM = 5.20 Am-1
KR1907
W/Up
N
550°C
350°C
NRM
NRM = 0.65 Am-1
KR2206
NRM = 1.47 Am-1
W/Up
N
550°C
350°C
NRM
KR2302
W/Up
N
560°C
350°C
NRM
NRM = 0.33 Am-1

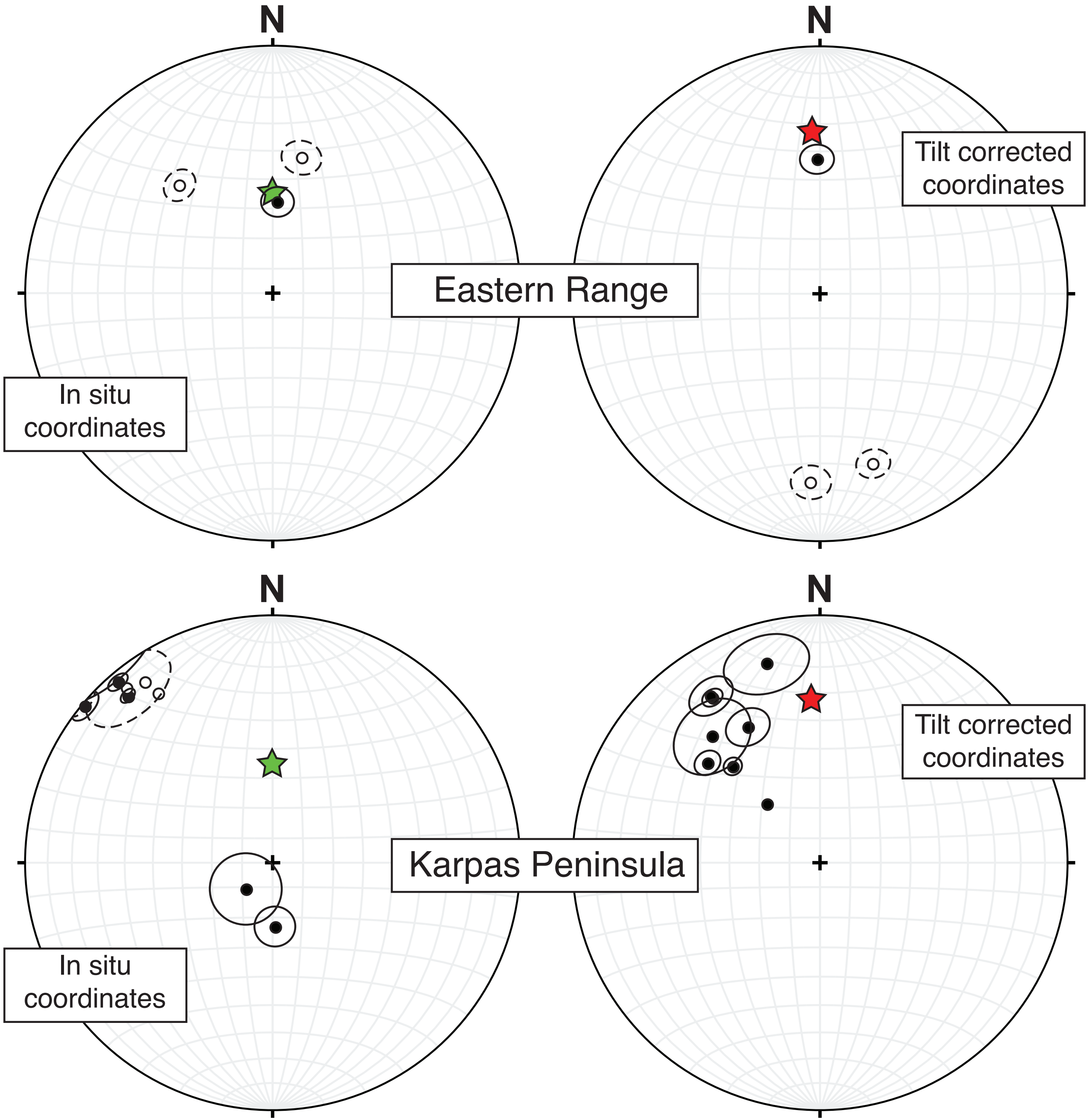
N
N
Tilt corrected coordinates
Eastern Range
In situ coordinates
N
N
Tilt corrected coordinates
Karpas Peninsula
In situ coordinates

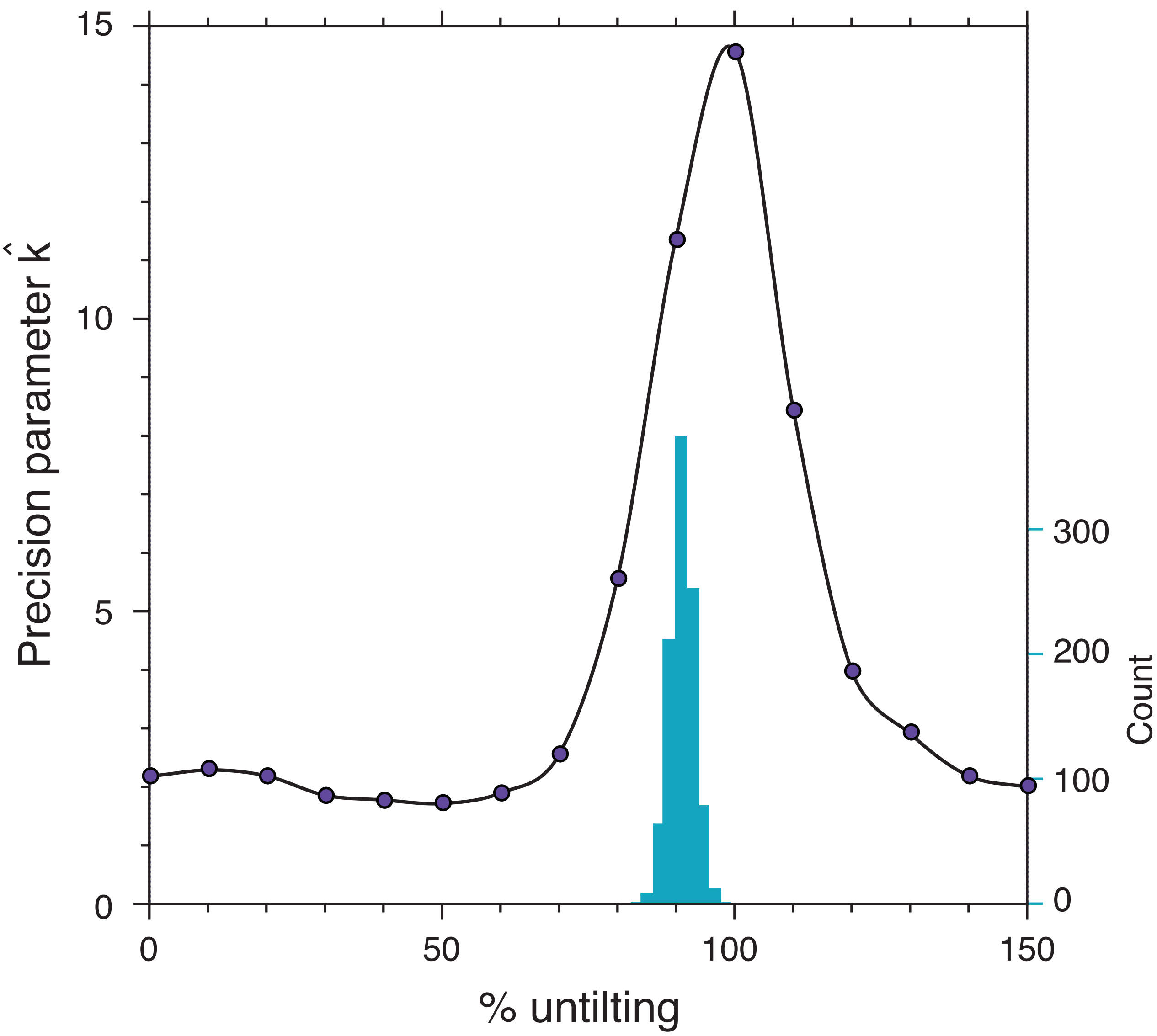

15
10
5
0
Precision parameter k̂
300
200
100
0
Count
0
50
100
150
% untilting

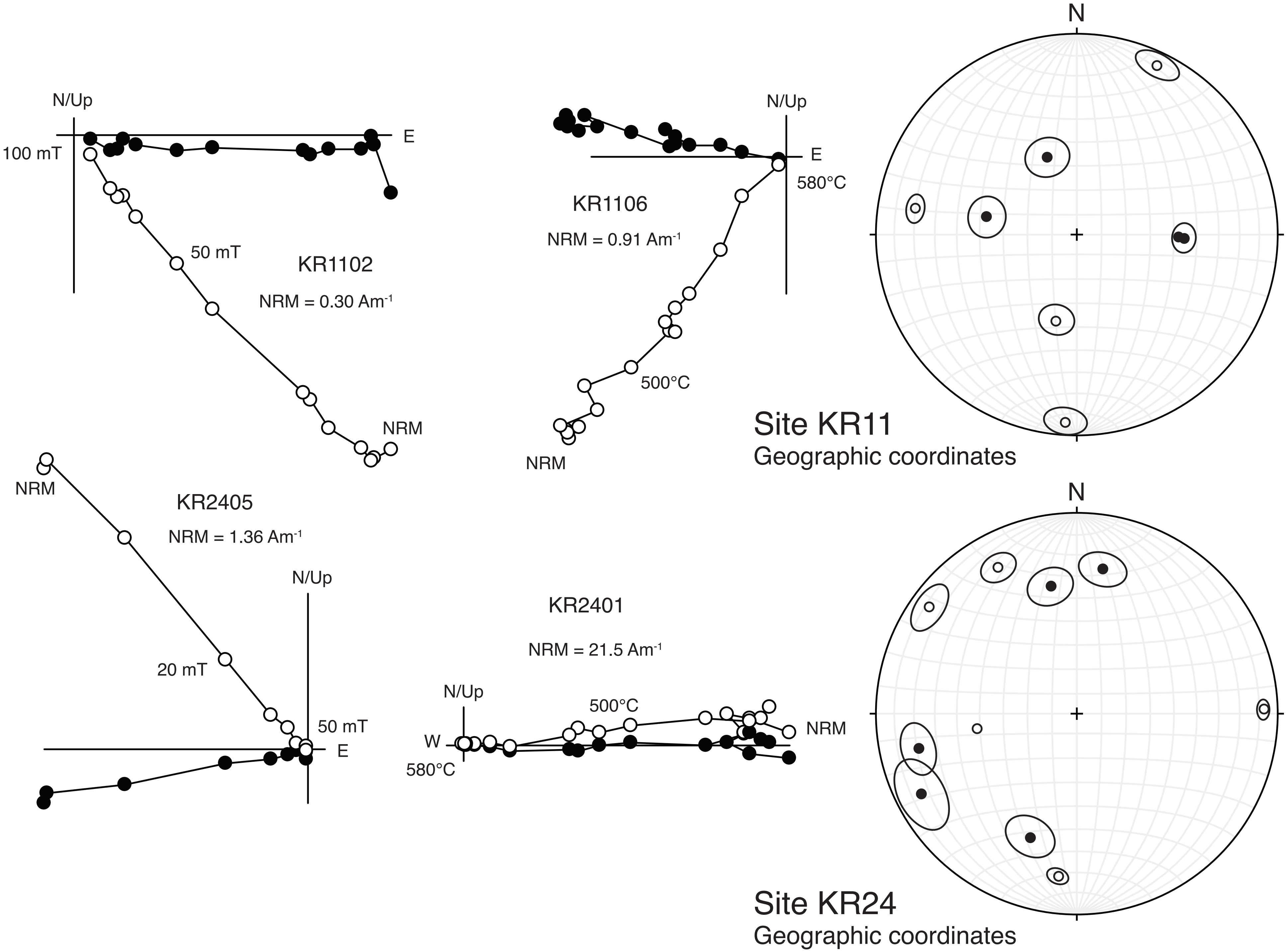
N/Up
E
100 mT
50 mT
KR1102
NRM = 0.30 Am-1
NRM
N/Up
E
580°C
KR1106
NRM = 0.91 Am-1
500°C
NRM
N
Site KR11
Geographic coordinates
NRM
KR2405
NRM = 1.36 Am-1
N/Up
20 mT
50 mT
E
KR2401
NRM = 21.5 Am-1
N/Up
500°C
W
NRM
580°C
N
Site KR24
Geographic coordinates

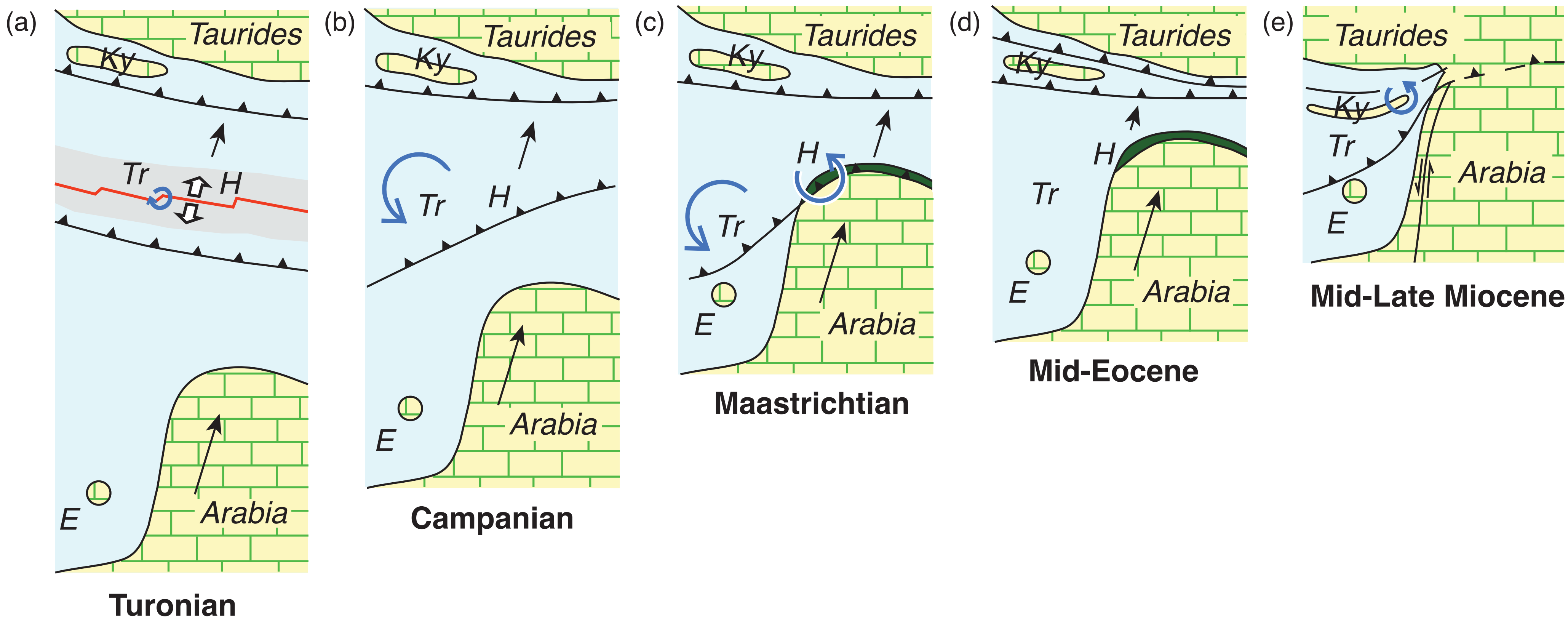

(a)
Taurides
Ky
Tr
H
E
Arabia
Turonian
(b)
Taurides
Ky
Tr
H
E
Arabia
Campanian
(c)
Taurides
Ky
H
Tr
E
Arabia
Maastrichtian
(d)
Taurides
Ky
H
Tr
E
Arabia
Mid-Eocene
(e)
Taurides
Ky
Tr
E
Arabia
Mid-Late Miocene